Supporting information

Enhanced photocatalytic activation of peroxodisulfate over Fe-containing MOF synthesized by single-crystal-to-single-crystal transformation for ofloxacin degradation

Hao Zhang,[a] Feng-Yu Chen,[a] Zhi-Yong Liu,[a] Yu-Hui Luo,[a,b,*] Zi-Lin Zhou,[a] Xue-Meng Jia,[a] Xin Wang,[a] Yun-Qiong Yang[a,*]

a *School of Environmental and Chemical Engineering, Jiangsu Ocean University, Lianyungang 222000, P. R. China.*

b *Jiangsu Institute of Marine Resources Development, Jiangsu Ocean University, Lianyungang 222000, P. R. China.*

* Corresponding authors. E-mail: luoyh@jou.edu.cn (Yu-Hui Luo),

yz9502@163.com (Yun-Qiong Yang)

Instruments

All samples were characterized by powder X-ray diffraction (PXRD; PANalytical X'pert PRO), Fourier transform infrared spectroscopy (FT-IR, Thermo Scientific equipment Nicolet iS10), scanning electron microscopy (SEM; Oxford JEOL JSM-7900F), thermogravimetric analysis (TGA, Netzsch TG 209 F1 Libra), or X-ray photoelectron spectroscopy (XPS). The Brunauer-Emmett-Teller (BET) surface areas of MOFs were determined using N_2 adsorption/desorption technique (BSD-PM1). Electron Spin Resonance (ESR, Bruker A200) tests were carried out to characterized the active radicals. The photoluminescence spectroscopy (PL, FL-7000 HITCAHI) was tested at room temperature with a Xenon lamp as a light source. Electrochemical and photocurrent dates were tested with a CHI660D electrochemical workstation (Shanghai Chenhua Instruments), a 300 W Xenon lamp was used as a light source. Photocatalytic experiments were carried out at an YCYN-GHX-D photochemical reactor (Shanghai Zhimei Instruments). The absorbance of solution was measured by an INESA L8 Plus UV-Vis spectrophotometer.

X-ray crystallography

Crystallographic diffraction data for In_3-TCA and Fe_2In-TCA were recorded on a Bruker D8 diffractometer with graphite monochromatized Mo-$K\alpha$ radiation (λ = 0.71073 Å) at 240 K. In_3-TCA and Fe_2In-TCA were solved by Direct Method of SHELXT-2016 and refined by full-matrix least-squares techniques by using the SHELXL-2018 program [1]. All nonhydrogen atoms were refined with anisotropic temperature parameters. All hydrogen atoms were placed in geometrically idealized position as a riding mode. The solvent molecules and NO_3^- anions in the crystal are highly disordered and are removed using the SQUEEZE routine of PLATON [2]. NO_3^- anions were added to the formular of MOF directly for charge balance. The number of solvent molecules cannot be accurately determined at present, so it has not been added to the Formula. CCDC number for In_3-TCA and Fe_2In-TCA is 2143113 and 2143114, respectively. The crystallographic data for In_3-TCA and Fe_2In-TCA were summarized in Table S2, and the selected bond lengths and angles are listed in Table S3 and S4.

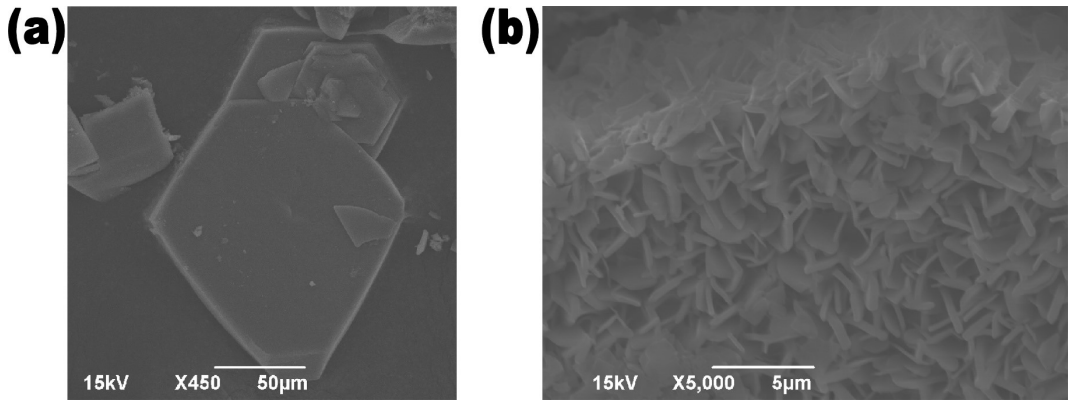

Fig. S1. SEM images of In_3-TCA prepared with the addition of 10 μL/mL (a) and 0 μL/mL (b) of HNO_3.

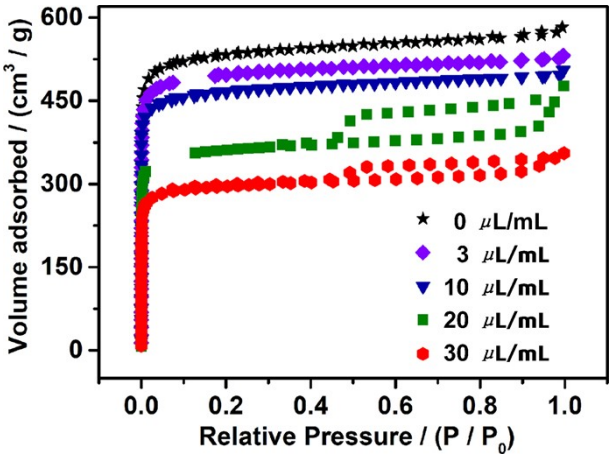

Fig. S2. Nitrogen adsorption/desorption isotherms of Fe_2In-TCA synthesized under different acidity.

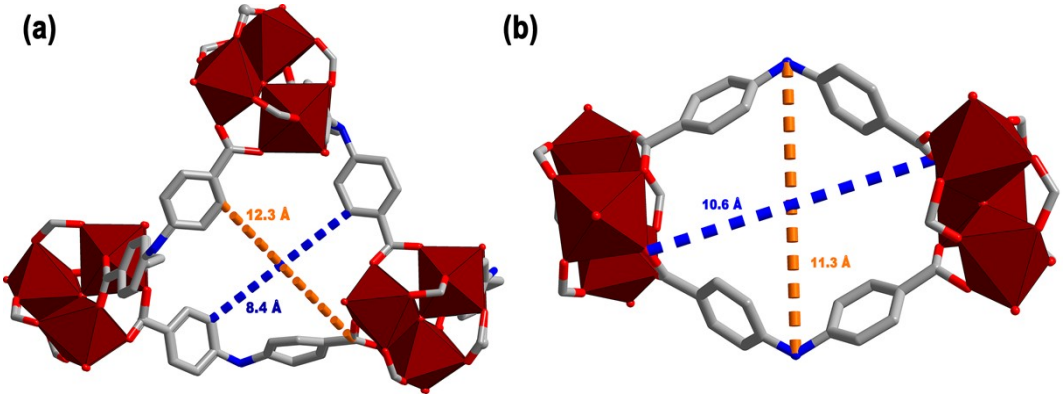

Fig. S3. Channel window size of Fe_2In-TCA.

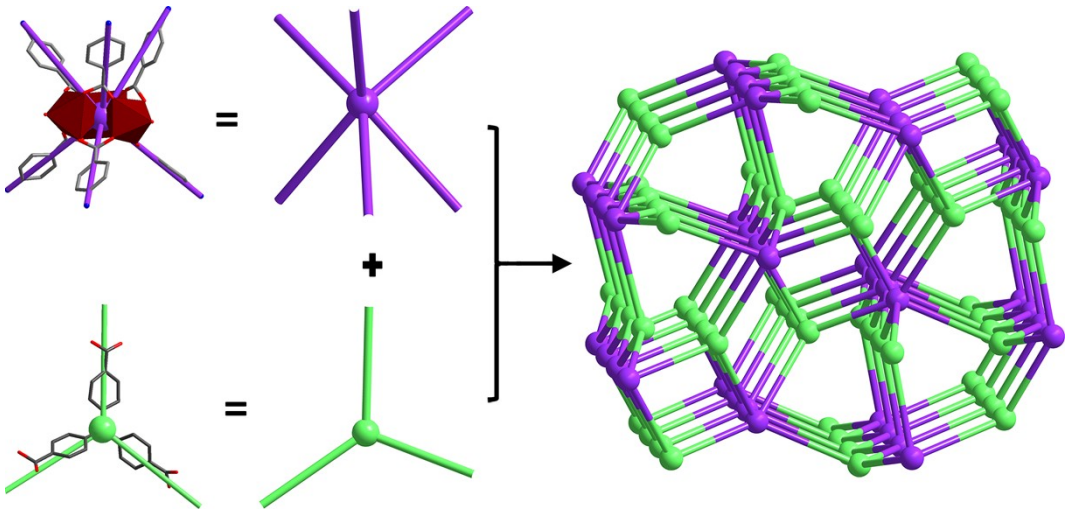

Fig. S4. Each trimeric SBU links to six TCA^{3-} can be defined as a six-connected node and each TCA^{3-} ligand coordinates to three trimeric SBUs can be defined as a three-connected node, then the framework of Fe_2In-TCA can be reduced to a new type of (3,6)-connected network.

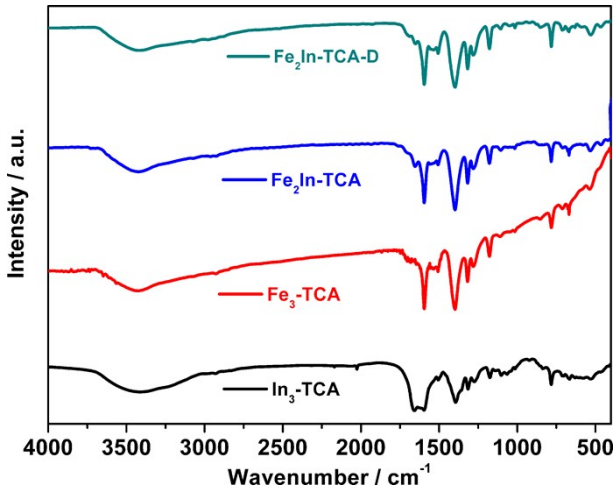

Fig. S5. FT-IR spectra of different MOFs.

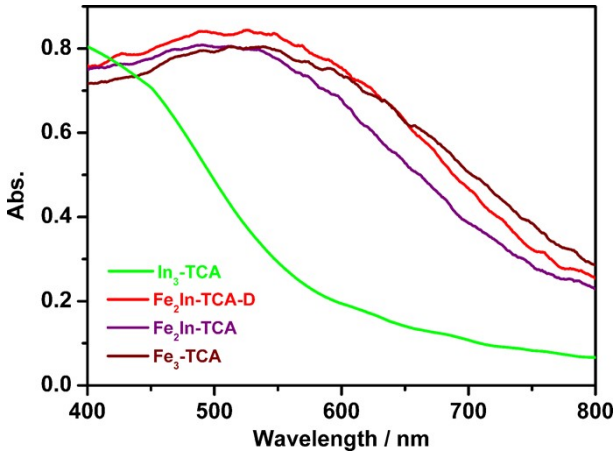

Fig. S6. Solid UV-vis absorption spectra of different MOFs.

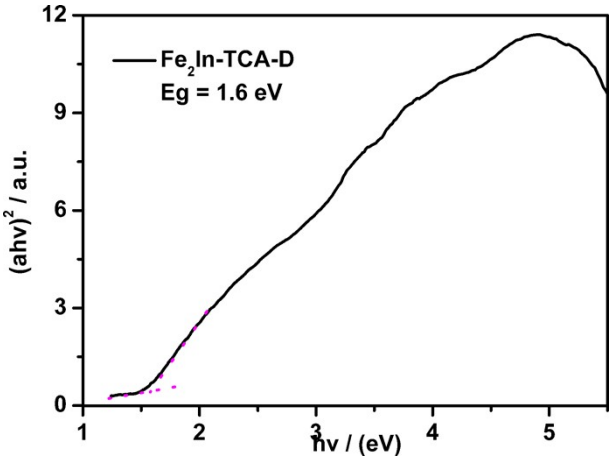

Fig. S7. UV-visible diffuse reflection and band gap of Fe_2In-TCA-D.

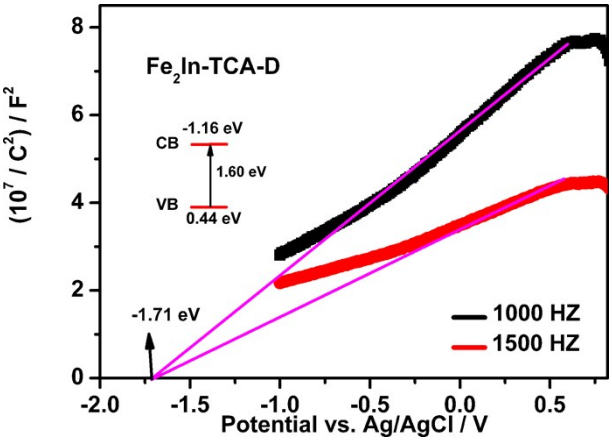

Fig. S8. Mott-Schottky plots Fe_2In-TCA-D. Inset: CB/VB potential of Fe_2In-TCA-D.

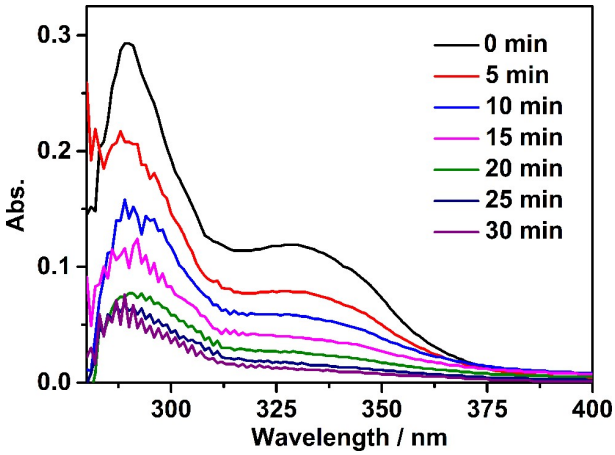

Fig. S9. Time-dependent absorption spectra of OFL solution in the presence of Fe_2In-TCA.

Table S1. Comparison of OFL degradation efficiency with different photocatalysts.

Catalysts	K (min^{-1})	Efficiency (%)	Time (min)	Light source	Peroxide	Reference
$BaTiO_3/WS_2$	0.173	89%	100	visible light	PS	Commun. Chem., 2022, 5, 95
Bi_2S_3/Bi_2WO_6	0.0112	87%	180	visible light	H_2O_2	Chem. Eng. J., 2018, 354, 692
$BiVO_4$/g-$C_3N_4/NiFe_2O_4$	0.1353	96%	60	visible light	/	Chem. Eng. J., 2021, 405, 126704
Co-MIL-53-NH-BT	0.0392	99.8%	140	visible light	/	J. Hazard. Mater., 2020, 387, 122011
Co-MoS_2	0.3121	91.1%	30	visible light	PMS	Chem. Eng. J., 2020, 401, 125978
$LaNiO_3$	0.061	97%	60	visible light	PMS	Chem. Eng. J., 2019, 359, 828
P_2-Mn_3O_4	0.667	99.5	10	ultraviolet light	PMS	Appl. Catal. B-Environ. 2019, 248, 298
Fe_2In-TCA	0.0815	98%	30	visible light	PDS	**This work**

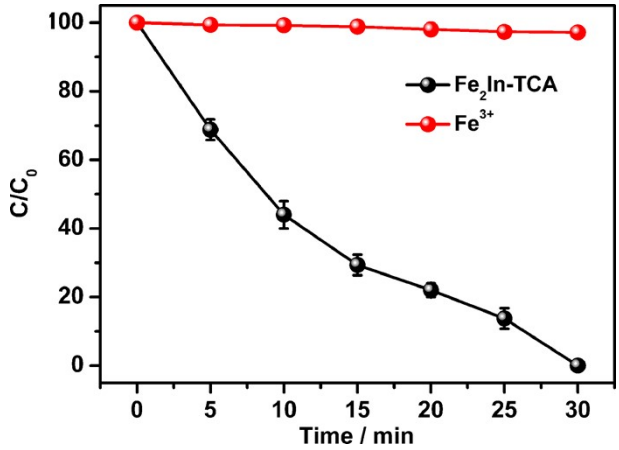

Fig. S10. Degradation of OFL in the presence of Fe_2In-TCA or Fe^{3+}.

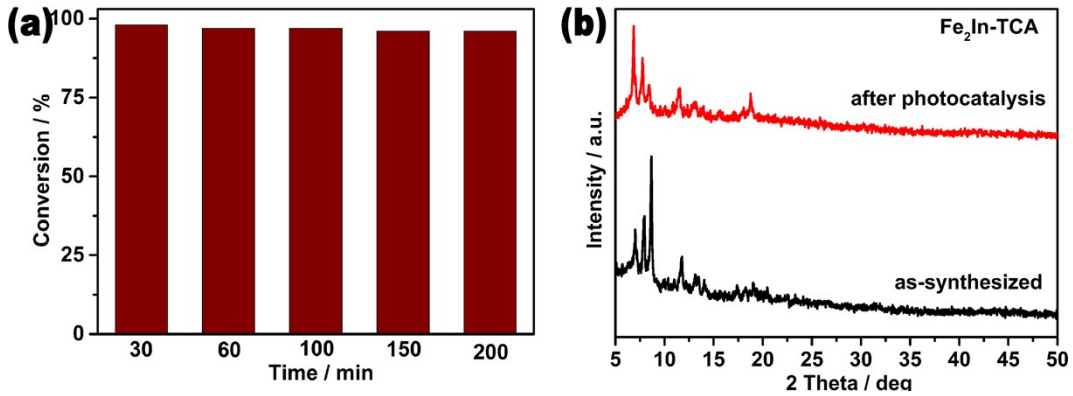

Fig. S11. (a) The circle experiment for removing OFL by Fe_2In-TCA. (b) The PXRD spectra of Fe_2In-TCA before and after photocatalytic reactions.

Table S2. Crystallographic data of In_3-TCA and Fe_2In-TCA.

Compounds	In_3-TCA	Fe_2In-TCA
Formula[a]	$C_{84}H_{60}In_6N_6O_{38}$	$C_{84}H_{60}Fe_4In_2N_6O_{38}$
Formula weight	2450.3	2214.42
Crystal system	orthorhombic	orthorhombic
Space group	*Pca2₁*	*Pca2₁*
a (Å)	31.248(4)	31.104(5)
b (Å)	16.2834(18)	16.117(2)
c (Å)	42.122(5)	41.896(7)
V (Å^3)	21433(4)	21003(6)
Z	4	4
Density (g cm^{-3})	0.759	0.7
μ / mm^{-1}	0.674	0.525
F(000)	4816	4448
2θ (°)	35.04	46.67
Reflections collected	71221	90692
Data/restraints/parameters	13596/3141/1064	29981/3134/992
GOF on F^2	1.01	1.049
R_1, wR_2 [I > 2σ (I)][b]	R_1 = 0.0558, wR_2 = 0.1332	R_1 = 0.0839, wR_2 = 0.179

[a] NO_3^- anions were added to the formular directly for charge balance. The number of solvent molecules cannot be accurately determined at present, so it has not been added to the formula.

[b] $R_1 = \sum||F_0| - |Fc||/\sum|F_0|$; $wR_2 = \sum[w(F_0^2 - Fc^2)^2]/\sum[w(F_0^2)^2]^{1/2}$.

Table S3. Selected bond lengths (Å) and angels (°) for In_3-TCA.

In_1-O_1	2.026(15)	In_1-O_{1w}	2.047(17)
In_1-O_{10}	2.148(19)	In_1-$O_{25}{}^1$	2.173(12)
In_1-$O_{12}{}^2$	2.218(15)	In_1-O_3	2.232(16)
In_2-O_1	2.092(16)	In_2-$O_{24}{}^3$	2.177(16)
In_2-O_{16}	2.186(16)	In_2-O_{2w}	2.152(15)
In_2-O_4	2.186(15)	In_2-$O_{11}{}^2$	2.256(19)
In_3-O_1	1.993(15)	In_3-$O_{26}{}^1$	1.904(13)
In_3-$O_{23}{}^3$	2.088(17)	In_3-O_9	2.179(17)
In_3-O_{15}	2.195(18)	In_3-O_{3w}	2.22(2)
In_4-O_2	2.016(15)	In_4-$O_6{}^4$	2.106(19)
In_4-O_{4w}	2.136(15)	In_4-O_{13}	2.164(17)
In_4-O_{21}	2.190(17)	In_4-$O_{20}{}^5$	2.203(14)
In_5-O_2	1.990(16)	In_5-O_{14}	2.108(19)
In_5-O_7	2.182(18)	In_5-$O_5{}^4$	2.217(15)
In_5-O_{5w}	2.187(18)	In_5-$O_{18}{}^6$	2.240(15)
In_6-$O_{17}{}^6$	1.772(18)	In_6-O_2	2.087(16)
In_6-O_{6w}	2.150(17)	In_6-$O_{19}{}^5$	2.159(16)
In_6-O_8	2.179(17)	In_6-O_{22}	2.172(18)

O_1-In_1-O_{1w}	178.7(7)	O_1-In_1-O_{10}	89.6(6)
O_{1w}-In_1-O_{10}	91.5(7)	O_1-In_1-$O_{25}{}^1$	90.5(6)
O_{1w}-In_1-$O_{25}{}^1$	88.6(6)	O_{10}-In_1-$O_{25}{}^1$	88.6(6)
O_1-In_1-$O_{12}{}^2$	93.5(6)	O_{1w}-In_1-$O_{12}{}^2$	85.4(7)
O_{10}-In_1-$O_{12}{}^2$	176.8(6)	$O_{25}{}^1$-In_1-$O_{12}{}^2$	90.6(6)
O_{1w}-In_1-O_3	84.6(7)	O_{10}-In_1-O_3	87.3(6)
$O_{25}{}^1$-In_1-O_3	172.0(6)	$O_{12}{}^2$-In_1-O_3	93.2(7)
O_1-In_2-$O_{24}{}^3$	98.3(6)	O_1-In_2-O_{16}	90.0(6)
$O_{24}{}^3$-In_2-O_{16}	91.8(7)	O_1-In_2-O_{2w}	177.4(6)
$O_{24}{}^3$-In_2-O_{2w}	84.2(6)	O_{16}-In_2-O_{2w}	89.0(7)
O_1-In_2-O_4	96.4(6)	$O_{24}{}^3$-In_2-O_4	88.3(7)
O_{16}-In_2-O_4	173.5(7)	O_{2w}-In_2-O_4	84.5(7)
O_1-In_2-$O_{11}{}^2$	91.9(7)	$O_{24}{}^3$-In_2-$O_{11}{}^2$	169.8(7)
O_{16}-In_2-$O_{11}{}^2$	89.2(7)	O_{2w}-In_2-$O_{11}{}^2$	85.7(7)
O_4-In_2-$O_{11}{}^2$	89.6(7)	O_1-In_3-$O_{26}{}^1$	90.2(6)
O_1-In_3-$O_{23}{}^3$	94.4(6)	$O_{26}{}^1$-In_3-$O_{23}{}^3$	173.8(6)
O_1-In_3-O_9	92.5(6)	$O_{26}{}^1$-In_3-O_9	90.0(7)
$O_{23}{}^3$-In_3-O_9	85.7(7)	O_1-In_3-O_{15}	94.0(6)
$O_{26}{}^1$-In_3-O_{15}	90.3(7)	$O_{23}{}^3$-In_3-O_{15}	93.5(7)
O_9-In_3-O_{15}	173.5(7)	O_1-In_3-O_{3w}	176.1(7)
$O_{26}{}^1$-In_3-O_{3w}	86.0(7)	$O_{23}{}^3$-In_3-O_{3w}	89.4(7)
O_9-In_3-O_{3w}	86.9(7)	O_{15}-In_3-O_{3w}	86.7(8)
O_2-In_4-$O_6{}^4$	89.5(7)	O_2-In_4-O_{4w}	176.9(7)
$O_6{}^4$-In_4-O_{4w}	88.3(7)	O_2-In_4-O_{13}	93.2(7)
$O_6{}^4$-In_4-O_{13}	85.6(7)	O_{4w}-In_4-O_{13}	88.7(6)
O_2-In_4-O_{21}	93.0(7)	$O_6{}^4$-In_4-O_{21}	91.7(7)
O_{4w}-In_4-O_{21}	85.0(6)	O_{13}-In_4-O_{21}	173.3(7)
O_2-In_4-$O_{20}{}^5$	94.8(6)	$O_6{}^4$-In_4-$O_{20}{}^5$	174.1(7)
O_{4w}-In_4-$O_{20}{}^5$	87.6(6)	O_{13}-In_4-$O_{20}{}^5$	90.1(6)
O_{21}-In_4-$O_{20}{}^5$	92.1(6)	O_2-In_5-O_{14}	90.9(7)
O_2-In_5-O_7	94.6(7)	O_{14}-In_5-O_7	84.8(7)
O_2-In_5-$O_5{}^4$	95.1(6)	O_{14}-In_5-$O_5{}^4$	89.2(7)
O_7-In_5-$O_5{}^4$	168.7(7)	O_2-In_5-O_{5w}	175.6(7)
O_{14}-In_5-O_{5w}	87.0(7)	O_7-In_5-O_{5w}	81.4(7)
$O_5{}^4$-In_5-O_{5w}	88.7(7)	O_2-In_5-$O_{18}{}^6$	98.1(6)
O_{14}-In_5-$O_{18}{}^6$	170.9(6)	O_7-In_5-$O_{18}{}^6$	93.1(6)
$O_5{}^4$-In_5-$O_{18}{}^6$	91.3(6)	O_{5w}-In_5-$O_{18}{}^6$	83.9(6)
$O_{17}{}^6$-In_6-O_2	95.1(7)	$O_{17}{}^6$-In_6-O_{6w}	86.4(7)
O_2-In_6-O_{6w}	177.5(7)	$O_{17}{}^6$-In_6-$O_{19}{}^5$	171.5(7)
O_2-In_6-$O_{19}{}^5$	93.3(6)	O_{6w}-In_6-$O_{19}{}^5$	85.3(6)
$O_{17}{}^6$-In_6-O_8	96.1(7)	O_2-In_6-O_8	89.3(6)
O_{6w}-In_6-O_8	88.6(7)	$O_{19}{}^5$-In_6-O_8	85.4(6)
$O_{17}{}^6$-In_6-O_{22}	86.2(7)	O_2-In_6-O_{22}	91.7(7)
O_{6w}-In_6-O_{22}	90.4(7)	$O_{19}{}^5$-In_6-O_{22}	92.2(6)

O_8-In_6-O_{22}	177.4(6)		

Symmetry transformations: [1] 1/2 - X, -1 + Y, 1/2 + Z; [2] -1/2 + X, -Y, +Z; [3] 1/2 - X, +Y, 1/2 + Z; [4] 1/2 + X, 1 - Y, +Z; [5] -X, -Y, -1/2 + Z; [6] -X, 1 - Y, -1/2 + Z.

Table S4. Selected bond lengths (Å) and angels (°) for Fe_2In-TCA.

Fe_1-O_1	1.947(14)	Fe_1-O_{12}	2.044(15)
Fe_1-O_{14}^1	2.163(13)	Fe_1-O_{24}^2	2.166(11)
Fe_1-O_5	2.143(14)	Fe_1-O_{1w}	2.216(13)
Fe_2-O_{23}^2	1.811(12)	Fe_2-O_{26}^3	2.087(11)
Fe_2-O_1	2.052(14)	Fe_2-O_{11}	2.150(14)
Fe_2-O_{15}	2.113(16)	Fe_2-O_{2w}	2.340(15)
In_3-O_1	2.097(13)	In_3-O_6	2.138(13)
In_3-O_{25}^3	2.161(12)	In_3-O_{13}^1	2.134(15)
In_3-O_{16}	2.197(15)	In_3-O_{3w}	2.177(13)
Fe_4-O_2	2.017(13)	Fe_4-O_{21}	2.069(14)
Fe_4-O_8^1	2.099(14)	Fe_4-O_{18}^5	2.118(13)
Fe_4-O_9	2.117(12)	Fe_4-O_{4w}	2.274(13)
Fe_5-O_2	2.050(14)	Fe_5-O_{22}	2.048(15)
Fe_5-O_{20}^6	1.971(13)	Fe_5-O_{17}^5	2.091(14)
Fe_5-O_4	2.129(13)	Fe_5-O_{5w}	2.186(14)
In_6-O_{10}	2.000(13)	In_6-O_2	2.010(14)
In_6-O_{19}^6	2.162(13)	In_6-O_7^4	2.176(12)
In_6-O_3	2.240(16)	In_6-O_{6w}	2.308(14)
O_1-Fe_1-O_{12}	88.6(6)	O_1-Fe_1-O_{14}^1	92.1(5)
O_{12}^1-Fe_1-O_{14}^1	176.5(6)	O_1-Fe_1-O_{24}^2	93.4(5)
O_{12}^1-Fe_1-O_{24}^2	89.9(5)	O_{14}^1-Fe_1-O_{24}^2	86.6(6)
O_1-Fe_1-O_5	94.4(6)	O_{12}-Fe_1-O_5	88.2(5)
O_{14}^1-Fe_1-O_5	95.2(6)	O_{24}^2-Fe_1-O_5	171.9(6)
O_1-Fe_1-O_{1w}	178.6(5)	O_{12}-Fe_1-O_{1w}	91.6(5)
O_{14}^1-Fe_1-O_{1w}	87.6(5)	O_{24}^2-Fe_1-O_{1w}	85.2(5)
O_5-Fe_1-O_{1w}	87.0(5)	O_{23}^2-Fe_2-O_{26}^3	175.3(6)
O_{23}^2-Fe_2-O_1	88.0(6)	O_{26}^3-Fe_2-O_1	92.7(5)
O_{23}^2-Fe_2-O_{11}	90.7(6)	O_{26}^3-Fe_2-O_{11}	84.7(6)
O_1-Fe_2-O_{11}	88.1(5)	O_{23}^2-Fe_2-O_{15}	88.0(6)
O_{26}^3-Fe_2-O_{15}	96.6(6)	O_1-Fe_2-O_{15}	93.6(6)
O_{11}-Fe_2-O_{15}	177.8(6)	O_{23}^2-Fe_2-O_{2w}	87.7(6)
O_{26}^3-In_2-O_{2w}	91.3(5)	O_1-Fe_2-O_{2w}	174.4(5)
O_{11}-Fe_2-O_{2w}	88.3(5)	O_{15}-Fe_2-O_{2w}	89.9(6)
O_1-In_3-O_6	92.9(5)	O_1-In_3-O_{25}^3	98.3(5)
O_6-In_3-O_{25}^3	87.3(6)	O_1-In_3-O_{13}^1	91.3(5)
O_6-In_3-O_{13}^1	88.4(6)	O_{25}^3-In_3-O_{13}^1	169.7(5)
O_1-In_3-O_{16}	92.0(6)	O_6-In_3-O_{16}	174.7(6)
O_{25}^3-In_3-O_{16}	90.1(6)	O_{13}^1-In_3-O_{16}	93.3(6)
O_1-In_3-O_{3w}	174.9(5)	O_6-In_3-O_{3w}	85.1(5)

O_{25}^{3}-In_3-O_{3w}	86.3(5)	O_{13}^{1}-In_3-O_{3w}	84.0(5)
O_{16}^{3}-In_3-O_{3w}	90.1(5)	O_2-Fe_4-O_{21}	94.4(6)
O_2-In_4-O_8^{4}	89.7(6)	O_{21}-In_4-O_8^{4}	87.0(6)
O_2-In_4-O_{18}^{5}	93.8(6)	O_{21}-In_4-O_{18}^{5}	95.6(6)
O_8-In_4-O_{18}^{5}	175.5(6)	O_2-In_4-O_9	91.6(5)
O_{21}-In_4-O_9	171.3(6)	O_8^{4}-In_4-O_9	86.9(6)
O_{18}^{5}-In_4-O_9	94.8(6)	O_2-In_4-O_{4w}	178.1(5)
O_{21}-In_4-O_{4w}	84.3(5)	O_8^{4}-In_4-O_{4w}	88.8(6)
O_{18}^{5}-In_4-O_{4w}	87.8(5)	O_9-In_4-O_{4w}	89.4(5)
O_2-Fe_5-O_{22}	95.5(6)	O_2-Fe_5-O_{20}^{6}	98.0(6)
O_{22}-Fe_5-O_{20}^{6}	86.7(6)	O_2-Fe_5-O_{17}^{5}	94.2(5)
O_{22}-Fe_5-O_{17}^{5}	93.1(6)	O_{20}^{6}-Fe_5-O_{17}^{5}	167.8(5)
O_2-Fe_5-O_4	88.8(5)	O_{22}-Fe_5-O_4	175.0(6)
O_{20}^{6}-Fe_5-O_4	95.2(6)	O_{17}^{5}-Fe_5-O_4	84.1(6)
O_2-Fe_5-O_{5w}	178.8(5)	O_{22}-Fe_5-O_{5w}	85.5(6)
O_{20}^{6}-Fe_5-O_{5w}	82.6(5)	O_{17}^{5}-Fe_5-O_{5w}	83.9(6)
O_4-Fe_5-O_{5w}	90.1(5)	O_{10}-In_6-O_2	85.0(6)
O_{10}-In_6-O_{19}^{6}	171.8(6)	O_2-In_6-O_{19}^{6}	99.1(5)
O_{10}-In_6-O_7^{4}	97.3(6)	O_2-In_6-O_7^{4}	95.5(5)
O_{19}^{6}-In_6-O_7^{4}	89.4(6)	O_{10}-In_6-O_3	79.6(5)
O_2-In_6-O_3	93.4(5)	O_{19}^{6}-In_6-O_3	93.0(5)
O_7^{4}-In_6-O_3	170.3(6)	O_{10}-In_6-O_{6w}	91.5(5)
O_2-In_6-O_{6w}	175.2(5)	O_{19}^{6}-In_6-O_{6w}	84.0(5)
O_{74}-In_6-O_{6w}	88.1(5)	O_3-In_6-O_{6W}	82.8(5)

Symmetry transformations: [1] 1/2 - X, -1 + Y, 1/2 + Z; [2] -1/2 + X, -Y, +Z; [3] 1/2 - X, +Y, 1/2 + Z; [4] 1/2 + X, 1 - Y, +Z; [5] -X, -Y, -1/2 + Z; [6] -X, 1 - Y, -1/2 + Z.

Reference

1. G.M. Sheldrick. Crystal structure refinement with SHELXL. *Acta Crystallogr. C.* 2015, 71, 3-8.
2. A.L. Spek. Single-crystal structure validation with the program PLATON. *J. Appl. Cryst.*, 2013, 3, 7-13.